Earth and Planetary Science Letters 503 (2018) 88–94

Contents lists available at ScienceDirect

Earth and Planetary Science Letters

www.elsevier.com/locate/epsl

Cooling rates of lunar orange glass beads

Hejiu Hui (惠鹤九)[a,*], Kai-Uwe Hess[b], Youxue Zhang (张有学)[c], Alexander R.L. Nichols[d], Anne H. Peslier[e], Rebecca A. Lange[c], Donald B. Dingwell[b], Clive R. Neal[f]

[a] State Key Laboratory for Mineral Deposits Research & Lunar and Planetary Science Institute, School of Earth Sciences and Engineering, Nanjing University, Nanjing, Jiangsu 210023, China
[b] Department of Earth and Environmental Sciences, LMU-University of Munich, Theresienstrasse 41/III, 80333 Munich, Germany
[c] Department of Earth and Environmental Sciences, University of Michigan, Ann Arbor, MI 48109, USA
[d] Department of Geological Sciences, University of Canterbury, Christchurch 8140, New Zealand
[e] Jacobs, NASA-Johnson Space Center, Mail Code X13, Houston, TX 77058, USA
[f] Department of Civil and Environmental Engineering and Earth Sciences, University of Notre Dame, Notre Dame, IN 46556, USA

ARTICLE INFO

Article history:
Received 9 April 2018
Received in revised form 11 September 2018
Accepted 16 September 2018
Available online xxxx
Editor: W.B. McKinnon

Keywords:
Moon
volcanic glass bead
cooling rate
heat capacity
glass transition
lunar atmosphere

ABSTRACT

It is widely accepted that the Apollo 17 orange glass beads are of volcanic origin. The degree of degassing of the glass beads depends on their cooling rates, so the estimation of volatile contents in the parental magmas of these lunar pyroclastic glasses also depends on the cooling rates. The cooling rate can be estimated using the calorimetric properties of the glass across the glass transition. In this study, a series of heat capacity measurements were carried out on hand-picked lunar volcanic orange glass beads during several cycles of heating to temperatures above their glass transition using a differential scanning calorimeter. The cooling rate of orange glass beads (sample 74220,867) was calculated to be 101 K/min using the correlation between glass cooling rates and fictive temperatures estimated from their heat capacity–temperature paths. This cooling rate is close to the lower end of the range that best fits the diffusion profiles of several volatile species in the glass beads, and at the upper end of the cooling-rate range recorded in glasses quenched subaerially on Earth. The cooling rate is likely to be controlled by the cooling environment (cooling medium) such that the lunar volcanic glass beads could have been cooled in a gaseous medium released from volcanic eruptions on the Moon, but not during "free flight" in vacuum. The existence of a gas medium suggests, in turn, that there may have been at least a short-lived or episodic atmosphere on the early Moon at around 3.5 Ga.

© 2018 Elsevier B.V. All rights reserved.

1. Introduction

Mare magmas erupted ~3.2–3.8 Ga ago on the Moon's surface as large flood basalts and/or fire fountaining (e.g., Shearer et al., 2006), the latter evidenced by the presence of volcanic glass beads resulting from rapid cooling of lunar magma. Magma cooling rate is a major factor controlling the solidification process, and one that could also affect its final volatile contents. The analyses of some of Apollo glass beads provided evidence that lunar mantle does contain water (e.g., Saal et al., 2008; Füri et al., 2014; Chen et al., 2015). The best estimates of water contents in the magma before eruption have been recalculated by fitting diffusion profiles in the lunar volcanic green (Apollo 15) and orange (Apollo 17) glass beads with cooling rates between 120 to 180 K/min used in the modeling (Saal et al., 2008). However, cooling rates of lunar volcanic glasses estimated from laboratory simulations and theoretical calculations can differ by several orders of magnitude from <60 to >6000 K/min (Arndt et al., 1979; Uhlmann et al., 1981; Fang et al., 1983; Arndt et al., 1984; Birnie and Dyar, 1986; Ni et al., 2017). This large range partially stems from the different cooling environments considered in the studies. Laboratory experiments have demonstrated that cooling environment (ambient temperature, cooling media, etc.) can affect the cooling rate dramatically (Xu and Zhang, 2002). However, it is difficult to infer the exact volcanic environment on the lunar surface when the volcanic glass beads formed with our current knowledge. It is very possible that the environments used for estimating cooling rates of lunar volcanic glass beads are different from the real situation on the early Moon (Uhlmann et al., 1974; Arndt et al., 1979; Needham and Kring, 2017; Saxena et al., 2017). Therefore, it is important to estimate the cooling rates directly from the volcanic glass beads returned by the Apollo missions.

* Corresponding author at: State Key Laboratory for Mineral Deposits Research& Lunar and Planetary Science Institute, School of Earth Sciences and Engineering, Nanjing University, Nanjing, Jiangsu 210023, China.
E-mail address: hhui@nju.edu.cn (H. Hui).

https://doi.org/10.1016/j.epsl.2018.09.019
0012-821X/© 2018 Elsevier B.V. All rights reserved.

The cooling rates of glasses can be inferred from their heat capacity (C_p) curves measured during heating (e.g., Moynihan et al., 1976). This method does not require the knowledge of the environment in which the glass formed. The formation of glass via cooling from a silicate melt occurs at the glass transition, across which the structure of the melt is frozen into that of the glass. The glass transition is a kinetic process and the glass transition temperature depends on the cooling rate (Dingwell and Webb, 1990). The glass records the kinetics of the glass transition during cooling and this can be used to infer the cooling rate of the melt across the glass transition. The enthalpy relaxation geospeedometer, involving measuring the heat capacity as a function of temperature (when the quenched glass is heated in a differential scanning calorimeter to a temperature above its glass transition), is often used to determine the glass cooling rate (Wilding et al., 1995). Uhlmann et al. (1974) carried out heat capacity measurements on Apollo 17 orange glass beads and determined their cooling rate to be >320 K/min. However, each heat capacity curve in the glass transition interval (~890–980 K) was modeled with only 10 data points obtained from calorimeter during heating (Uhlmann et al., 1974). Now, in a state-of-the-art differential scanning calorimeter, heat capacities can be continuously measured. Furthermore, no quantitative method was applied to calculate the cooling rate of orange glass beads, and thus the previously measured cooling rate of >320 K/min was only semi-quantitative at best (Uhlmann et al., 1974).

The enthalpy relaxation geospeedometer has been widely used to calculate the cooling rates of natural silicate glasses that formed in different terrestrial environments, such as submarine (Wilding et al., 2000; Potuzak et al., 2008; Nichols et al., 2009), subglacial (Wilding et al., 2004), subaerial (Wilding et al., 1995, 1996a; Gottsmann and Dingwell, 2001, 2002), and even during impact events (Wilding et al., 1996b). The cooling rates of these natural glasses vary from $\sim 10^{-3}$ up to 10^{7} K/min (Gottsmann and Dingwell, 2002; Potuzak et al., 2008). Two methods have been developed to infer glass cooling rates from the heat capacity curves determined during heating using a differential scanning calorimeter: The Tool–Narayanaswamy enthalpy relaxation (T–N) geospeedometer (e.g., Tool, 1946; Narayanaswamy, 1971, 1988; DeBolt et al., 1976; Wilding et al., 1995), and the combined Moynihan–Yue area-matching approach (e.g., Moynihan et al., 1976; Yue et al., 2002; Potuzak et al., 2008; Nichols et al., 2009). The latter method can be applied to glass that cooled at any rate, but the T–N geospeedometer may be unable to fit heating C_p curves of rapidly quenched glasses (e.g., Potuzak et al., 2008; Nichols et al., 2009).

In this study, we report heat capacity measurements on the Apollo 17 orange glass beads. The results will be used to estimate the cooling rate of glass beads using the combined Moynihan–Yue area-matching approach (e.g., Moynihan et al., 1976). The calculated cooling rate of the glass beads is a key parameter in estimating the initial water contents of the glass-forming melts prior to eruption based on water concentration profiles in glass beads (Saal et al., 2008), which has an influence over the lunar mantle melting temperature, magma crystallization temperature and the style of volcanic eruption. Furthermore, the data can allow us to make some inferences about the lunar surface environment during the volcanic eruptions and to understand post-depositional processes such as welding, vesiculation, degassing and crystallization, which are in large part controlled by the thermal evolution of the glass within the volcanic deposit. Finally, the atmospheric conditions on the early Moon may have been influenced by volcanic eruptions (e.g., Needham and Kring, 2017; Neal, 2017) and our results have implications for the lunar atmosphere at the time of volcanic eruption.

Table 1
Chemical compositions of different groups of the Apollo 15 green glass beads (15421) and the Apollo 17 orange glass beads (74220).

	Green A	Green B	Green C	Green D	Green E	74220
SiO_2	45.5	46.0	48.0	45.1	45.2	38.5
TiO_2	0.38	0.40	0.26	0.41	0.43	9.12
Al_2O_3	7.75	7.92	7.74	7.43	7.4	5.8
FeO	19.7	19.1	16.5	20.3	19.8	22.9
MnO	0.22	n.a.	0.19	0.22	0.22	n.a.
MgO	17.2	17.2	18.2	17.6	18.3	14.9
CaO	8.65	8.75	8.57	8.43	8.15	7.40
Na_2O	n.d.	n.d.	n.d.	n.d.	n.d.	0.4
K_2O	n.d.	n.d.	n.d.	n.d.	n.d.	n.d.
Cr_2O_3	0.56	0.55	0.57	0.55	0.54	0.69
total	99.96	99.92	100.03	100.04	100.08	99.68

n.a. = not analyzed; n.d. = not detected. The compositions starting with "Green" are for different groups of the Apollo 15 green glass beads. The data presented here were compiled by Delano (1986).

2. Lunar volcanic glass beads

Lunar volcanic glass beads from Apollo 17 orange soil sample 74220,867 were used in this study. Various scenarios have been proposed to explain the formation of these glass beads (Roedder and Weiblen, 1973; Heiken et al., 1974; Meyer et al., 1975). The surfaces of the glass beads are coated by thin films composed of Zn, Ga, Pb, Cu, Tl, S, F, Cl, and other volatile elements (Meyer et al., 1975). It has been proposed that these elements were condensed as a sublimate on the bead surfaces during lava fountain eruptions (e.g., Meyer et al., 1975; Heiken and McKay, 1977; Reed et al., 1977; Clanton et al., 1978). This suggests that the Apollo 17 orange glass beads were produced by gas-charged fire fountain volcanic eruptions (Heiken et al., 1974; Meyer et al., 1975; Delano, 1986; Rutherford and Papale, 2009). A brief summary of sample characterization of 74220, from which sample 74220,867 was separated, is presented here.

Orange soil 74220, collected from the rim of Shorty Crater in the Taurus–Littrow region during the Apollo 17 mission, contains mainly orange glass spherules ranging from <1 μm to ~1 mm and broken fragments of the spherules, with minor amounts of basalt fragments (Heiken et al., 1974). Some of the orange glass beads are partially crystallized. The chemical compositions of the 74220 orange glass beads are homogeneous (Table 1, Heiken et al., 1974; Delano, 1986), as are their textures (Heiken et al., 1974). Compared with the Apollo 15 green glass beads, the 74220 orange glass beads have higher TiO_2 and FeO contents, but lower SiO_2, Al_2O_3, MgO, and CaO contents (Table 1; Delano, 1986). The ^{40}Ar–^{39}Ar age has been measured on five single orange glass beads from soil 74220, which gave a preferred age of 3.60 ± 0.04 Ga for their formation (Huneke, 1978). This is at the lower end of ^{87}Rb–^{87}Sr age range of 3.64–3.84 Ga measured in the Apollo 17 mare basalts (Nyquist, 1977). However, it is older than the ^{207}Pb–^{206}Pb age of 3.48 ± 0.03 Ga for 74220 (Tera and Wasserburg, 1976). The ages of orange glass beads are within error of the Apollo 15 green glass beads, which also resulted from lava fountain eruption (e.g., Chou et al., 1975; Heiken et al., 1974). A ^{207}Pb–^{206}Pb age for the interior of the green glass beads is 3.41 ± 0.33 Ga (Tatsumoto et al., 1987), and ^{40}Ar–^{39}Ar ages for the Groups A and D green glass beads are 3.41 ± 0.12 Ga and 3.35 ± 0.18 Ga respectively (Spangler et al., 1984).

3. Heat capacity measurements

Samples of the lunar soil 74220,867 were immersed in ethanol and individual intact and broken transparent glass beads were hand-picked under a binocular microscope. The selected grains are typically larger than 40 μm as these could be handled with tweezers. Consequently, the coarse fraction of the glass grains is overrep-

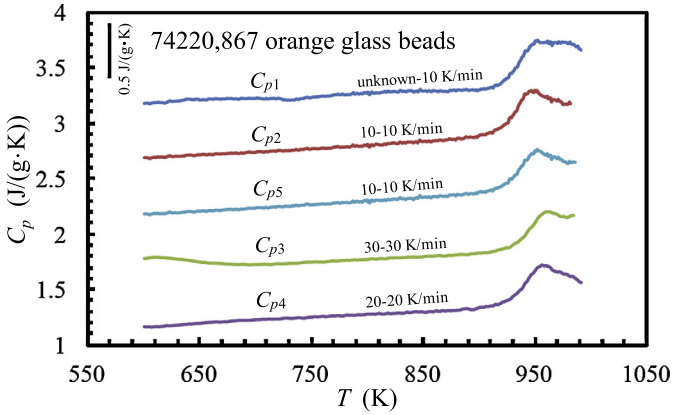

Fig. 1. Series of heat capacity (C_p) curves measured in the DSC during heating of the 74220,867 lunar orange glass beads. The curves are shifted vertically for clarity. Following the experimental sequence, the curves C_{p1-5} refer to: (1) initial reheating at 10 K/min of the raw glass beads cooled on the Moon's surface (C_{p1}), (2) reheating at 10 K/min of glass cooled at 10 K/min (C_{p2}), (3) reheating at 30 K/min of glass cooled at 30 K/min (C_{p3}), (4) reheating at 20 K/min of glass cooled at 20 K/min (C_{p4}), and (5) reheating at 10 K/min of glass cooled at 10 K/min (C_{p5}). The controlled cooling/reheating cycles (i.e., curves C_{p2-5}) enable the cooling rate and the glass fictive temperature to be correlated (see text for details).

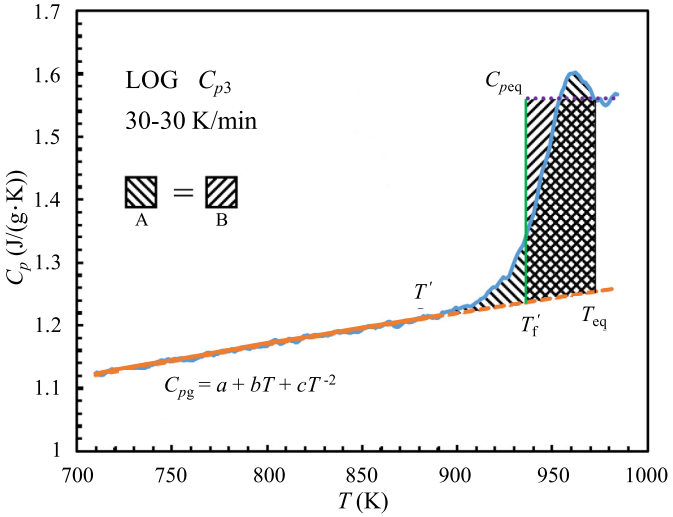

Fig. 2. Determination of fictive temperature (T'_f) for the heating C_p curves with known matching cooling and heating rates using the method of Moynihan et al. (1976). This C_p curve was obtained during heating at 30 K/min, after cooling at the same rate for the 74220,867 lunar orange glass beads (curve C_{p3} in Fig. 1). T'_f is defined as the temperature required for area A to equal area B. Area A is the left-hand side of Eq. (1), and area B is the right-hand side. The portion of C_p curve for the glass state (C_{pg}) was fit with Eq. (2) shown as the dashed line. The dotted line represents equilibrium C_p in the liquid state (C_{peq}).

resented whereas the extremely fine ones are under-represented. The selected beads were cleaned using ethanol and dried at room temperature. The cleaned glass beads of the soil sample 74220,867 were carefully loaded into a Pt crucible for heat capacity measurements.

The specific heat capacities (C_p) of the 74220,867 orange glasses during heating and cooling were determined using a differential scanning calorimeter (Netzsch® 404C Pegasus DSC) in the Department of Earth and Environmental Sciences, LMU-University of Munich. The C_p measurements generally followed the procedure outlined by Potuzak et al. (2008) and Nichols et al. (2009). A complete C_p measurement for the sample consists of a baseline measurement (two empty Pt crucibles covered with Pt lids), sapphire standard measurement (one crucible containing the 27.77 mg sapphire standard and the other empty, both covered with Pt lids), and sample measurement (one crucible containing the sample and the other empty, both covered with Pt lids). The mass of the glass grains measured here was 27.81 mg for sample 74220,867, comparable to that of the sapphire standard. The crucible containing glass beads was placed on the DSC sample holder at room temperature. The DSC was fluxed using ultrapure argon with a constant flow rate of 25 ml/min to prevent oxidation of the samples during the heat capacity measurements. The glass beads were initially held at 313 K, and then heated at 10 K/min through the glass state and the glass transition, after which the samples underwent further cooling and heating scans at 30 K/min, 20 K/min, and 10 K/min, where the heating rate matched the preceding cooling rate. After DSC measurements, some glass beads were polished and their interior textures were examined using a petrographic microscope. No obvious crystallization was observed within the beads.

The C_p curves of lunar volcanic glass beads at different cooling/heating cycles were calculated using all of the heat flow data from the baseline, standard, and sample measurements, the masses of the standard and sample, and the known heat capacity curve of the sapphire standard from Archer (1993). The errors of heat capacity are ±1% for the glass, and ±3% for the metastable liquid, respectively (Potuzak et al., 2008). The C_p curves determined using the DSC during the initial heating of natural volcanic glass beads and subsequent heating after cooling at the same controlled rates are shown in Fig. 1. Note that the initial heating C_{p1} curve for natural glass beads corresponds to average heat capacities of many grains with different sizes, which might have cooled at different rates on the Moon's surface. The main peak is wider than usual (curve C_{p1}, Fig. 1), which is almost certainly due to the relaxation of first slowly cooled (e.g., larger) and then more rapidly cooled (e.g., smaller) glass beads. Another feature on the C_{p1} curve measured during initial heating of sample 74220,867 orange glass beads is the wide and irregular trough from 690 to 900 K (Fig. 1).

4. Determination of fictive temperatures and cooling rate of lunar orange glass beads

The structural configuration of glass results from its thermal history, which can be deciphered using the enthalpy variation at the glass transition. Fictive temperature, a temperature at which the extrapolated enthalpy (or volume) of the glass intersects that of the liquid, is defined as the temperature at which the quenched structural state (configuration) of the glass would be the same as that of the liquid in metastable equilibrium (e.g., Tool, 1946; Dingwell and Webb, 1990; Ochs and Lange, 1997; Nichols et al., 2009). The fictive temperature of the glass is correlated with the cooling rate during glass formation. Operationally, the fictive temperature of a quenched glass can be determined from the structural relaxation of the glass to a new equilibrium as it is reheated. The continuous scan of heat capacity at constant pressure (C_p), the partial derivative of enthalpy, with respect to temperature can be used to study the relaxation process of enthalpy (e.g., Wilding et al., 1995) and the fictive temperature can be calculated from the C_p curve determined using a DSC during reheating of the glass.

The Tool–Narayanaswamy (T–N) enthalpy relaxation geospeedometer (e.g., Tool, 1946; Narayanaswamy, 1971, 1988; Wilding et al., 1995) has been widely used to calculate the cooling rates of volcanic glasses from heat capacity data (Wilding et al., 1995, 1996a, 2000, 2004; Gottsmann and Dingwell, 2001, 2002; Potuzak et al., 2008; Nichols et al., 2009). However, the T–N geospeedometer method does not apply well to our data of the C_p curves on heating of sample 74220,867 for the following reasons. First, both the lack of a trough and the presence of a small peak above the heat capacity at the equilibrium state (C_{peq} in Fig. 2) in heating C_p curves of glass beads with known cooling rates (curves C_{p2-5} in Fig. 1) are difficult to reproduce on the same curve us-

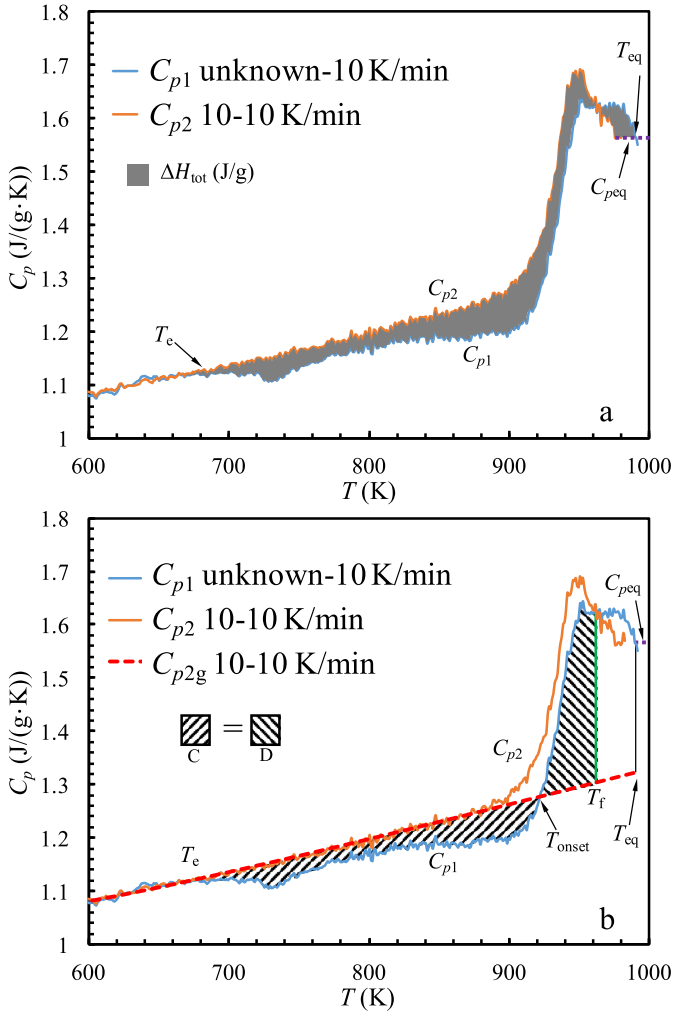

Fig. 3. Determination of fictive temperature (T_f) for the initial heating C_p curve (curve C_{p1} in Fig. 1) using a modified version of the method of Yue et al. (2002). (a) Graphical illustration of ΔH_{tot} of the 74220,867 lunar orange glass beads (the enthalpy stored in the glass during the natural quench on the Moon's surface) released during the initial heating, i.e., Eq. (4). (b) The fictive temperature (T_f) is defined as the temperature required for area C to equal area D. Area C is the left-hand side of Eq. (6), and area D is the right-hand side. Curve C_{p2g} is the Maier–Kelley curve fit for the glass state of curve C_{p2} with matched cooling and heating rates of 10 K/min (Fig. 1).

ing the T–N geospeedometer (e.g., Gottsmann and Dingwell, 2002; Nichols et al., 2009). Secondly, the C_p curve obtained during the initial heating of the naturally cooled glass beads (curve C_{p1} in Fig. 3a) contains a wide trough, and the peak at the glass transition is wider than usual, which are also difficult to model using the T–N geospeedometer.

An alternative method, the combined Moynihan–Yue area-matching approach (Moynihan et al., 1976; Yue et al., 2002), has been used to determine the average fictive temperature following the procedure of Potuzak et al. (2008) and Nichols et al. (2009). We briefly describe this method here and apply it to the C_p curves of the 74220,867 orange volcanic glass beads measured during heating. For a complete description see Moynihan et al. (1976), Yue et al. (2002), Potuzak et al. (2008), and Nichols et al. (2009).

4.1. Fictive temperature of lunar glass beads cooled at controlled rates

Following the procedure described in Potuzak et al. (2008) and Nichols et al. (2009), a correlation between fictive temperature and cooling rate has to be established first to infer the cooling rate of the volcanic glass beads that formed on the Moon's surface. This was carried out using the C_p measured on heating the glass beads at a known rate after cooling at the same rate (curves C_{p2-5} in Fig. 1). The equation to calculate the fictive temperature (Moynihan et al., 1976), which can be typically used for the glass cooled at a relatively slow rate, is:

$$\int_{T'}^{T_{eq}} (C_p - C_{pg})dT = \int_{T'_f}^{T_{eq}} (C_{peq} - C_{pg})dT, \quad (1)$$

where C_{pg} is the heat capacity of the glass including the extrapolated part (dashed line in Fig. 2), T_{eq} is the temperature at which the melt reaches equilibrium, T' is the temperature at which C_p deviates from C_{pg} of the glass, T'_f is the fictive temperature, T is the temperature, and C_{peq} is the heat capacity at the equilibrium state, which is the same for all measurements (Fig. 2). The heat capacity of the glass state, C_{pg}, is calculated using the Maier–Kelley curve equation:

$$C_{pg} = a + bT + cT^{-2}, \quad (2)$$

where a, b, and c are fitting parameters (Fig. 2). These three constants can be obtained by fitting the almost linearly increasing C_p curve on the low temperature side of the peak. A graphic illustration of Eqs. (1) and (2) is shown in Fig. 2, and T'_f in Eq. (1) is graphically defined as the temperature required for area A (left-hand side of Eq. (1)) to equal area B (right-hand side of Eq. (1)). This can be performed for each heating C_p curve with known matching cooling and heating rates (curves C_{p2-5} in Fig. 1). Therefore, a correlation between fictive temperature T'_f and cooling rate is established. The linear relationship between the logarithm of cooling rate and the reciprocal of T'_f has been found to be valid for a variety of glasses cooled at a wide range of quench rates (e.g., Moynihan et al., 1976; Nichols et al., 2009). However, Eq. (1) cannot be applied to a glass for which the C_p curve measured on heating has a trough that results from a fast quench, such as that on the C_p curve measured on initial heating of the 74220,867 orange glass beads (Fig. 1). Under such circumstances, a different method has to be applied.

4.2. Fictive temperature of naturally cooled lunar volcanic glass beads

The sample used in this study consists of thousands of orange glass beads, which may not have been cooled at the same rate on the Moon's surface. Therefore, the C_p curve determined for the 74220,867 orange glass beads during initial heating (curve C_{p1} in Figs. 1 and 3) represents a weighted average of the heat capacities of all the individual glass beads. The wide and irregular trough and wide peak may result from the beads having been quenched at different cooling rates. Note that all glass beads were cooled at the same rate after initial heating at 10 K/min during the heat capacity measurements. The trough in the C_{p1} curve across the glass transition interval indicates that enthalpy stored during cooling on the Moon's surface was released during the initial heating at 10 K/min (Figs. 1 and 3). The difference between the initial C_{p1} curve and the C_p curve also measured during heating at 10 K/min, but after the glass beads were cooled at 10 K/min (curves C_{p2} or C_{p5} in Figs. 1 and 3) is the enthalpy, ΔH, released by the glass at temperature, T, and ambient pressure, p:

$$(\partial \Delta H/\partial T)_p = C_{p2} - C_{p1}, \quad (3)$$

and the total enthalpy, ΔH_{tot}, released during the heating process can be calculated using

$$\Delta H_{\mathrm{tot}} = \int_{T_e}^{T_{eq}} \frac{\partial \Delta H}{\partial T} dT = \int_{T_e}^{T_{eq}} (C_{p2} - C_{p1}) dT, \quad (4)$$

where T_e is the temperature at which the release of enthalpy starts. This is graphically illustrated in Fig. 3a. Following Yue et al. (2002), Potuzak et al. (2008), and Nichols et al. (2009), for glasses that have undergone a fast quench, ΔH_{tot} is related to the total excess internal energy of the glass released between T_e and T_{eq} and the integral of the average inherent structural energy of the glass between T_{onset}, the temperature at which C_{p1} equals the heat capacity of the glass state of C_{p2} calculated using Eq. (2) (C_{p2g}) in the glass transition interval, and T_f, the fictive temperature of the naturally quenched glass, resulting in

$$\int_{T_e}^{T_{onset}} (C_{p2g} - C_{p1}) dT = \int_{T_{onset}}^{T_{eq}} (C_{p1} - C_{p2g}) dT + \int_{T_{eq}}^{T_f} (C_{peq} - C_{p2g}) dT. \quad (5)$$

As the integral between C_{p2g} and C_{p1} from T_e to T_{onset} is relatively small for the 74220,867 orange volcanic glass beads (Fig. 3b), the second component of the right-hand side of the equation is not required because the two sides of the equation match before T_{eq} is reached. As a result, Eq. (5) can be written as

$$\int_{T_e}^{T_{onset}} (C_{p2g} - C_{p1}) dT = \int_{T_{onset}}^{T_f} (C_{p1} - C_{p2g}) dT, \quad (6)$$

for the 74220,867 orange volcanic glass beads. A graphical illustration of Eq. (6) is shown in Fig. 3b, in which area C and D represent the left-hand and right-hand side of Eq. (6), respectively. Matching areas C and D gives a fictive temperature T_f of 962 K (961 K if curve C_{p5} is used instead of curve C_{p2}, Fig. 1) for the naturally cooled 74220,867 orange volcanic glass beads (Fig. 3b). This T_f is the average fictive temperature of all glass beads that are measured.

4.3. Determination of cooling rate of lunar orange glass beads

The fictive temperature T_f determined using the initial heating C_{p1} curve (Fig. 3) can be used to infer the cooling rate of the 74220,867 orange glass beads if a correlation between the fictive temperature and the cooling rate is established for the samples. Using the C_p curves with known matched cooling and heating rates (curves C_{p2-5} in Fig. 1), a linear relationship between the logarithm of the cooling rate and the reciprocal of fictive temperature T_f' determined with the area-matching approach (Fig. 2) can be established for the 74220,867 orange glass beads (Fig. 4). The extrapolation of this linear relationship to fictive temperature T_f gives an average cooling rate of 101 K/min for the 74220,867 natural orange glass beads (Fig. 4).

5. Discussion

5.1. Comparison of cooling rates obtained for lunar volcanic glass beads

Various studies have been carried out to infer lava cooling rates on the Moon's surface (e.g., Uhlmann et al., 1974; Donaldson et al., 1977; Arndt et al., 1984; Arndt and von Engelhardt, 1987). Textural analyses have shown that these volcanic glass beads have to be cooled at rates significantly slower than $8 \cdot 10^4$ K/min, which is the rate of "free flight" radiative cooling for glass beads of similar size (Arndt and von Engelhardt, 1987). The minimum cooling rate at which green glass melt solidifies as glass without detectable crystallization has been suggested to be ~60 K/min based on laboratory cooling experiments (Arndt et al., 1984), although this critical cooling rate may not be the same for the orange glasses, which are compositionally different from those of the green glass beads (Table 1). Ni et al. (2017) estimated the cooling rate of individual olivine crystals (~200 μm in diameter, larger than the average diameter of the glass beads in this study) in orange glass samples to be 60 ± 3 K/min or lower by comparing the trend of diffusive H loss in natural melt inclusions with those in experimentally-heated melt inclusions. Both results of Arndt et al. (1984) and Ni et al. (2017) are consistent with an average cooling rate of 101 K/min obtained for the 74220,867 volcanic glass beads.

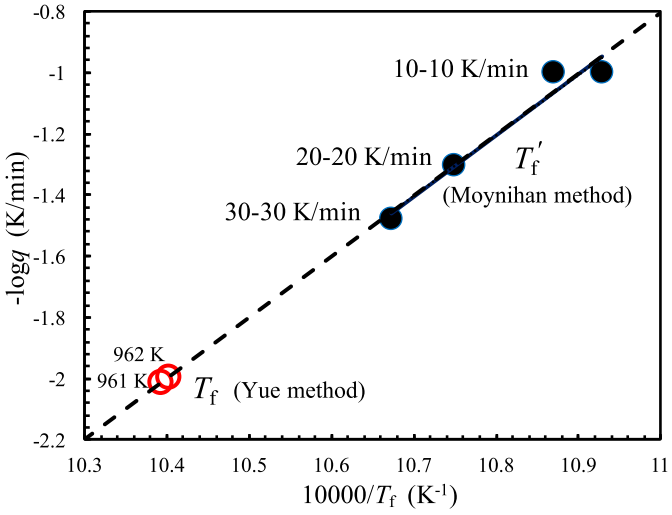

Fig. 4. Determination of the natural cooling rate of the 74220,867 lunar orange glass beads using the relationship between cooling rate and fictive temperature (T_f') calculated following the method of Moynihan et al. (1976) for the C_p curve with known matched cooling and heating rates (Fig. 2). This relationship is extrapolated to T_f determined for the initial heating C_p curve using the method of Yue et al. (2002) (Fig. 3) to calculate the natural cooling rate.

A previous calorimetric study of the 74220 orange glass has suggested that this material cooled at a rate exceeding 320 K/min across the glass transition region (Uhlmann et al., 1974), which is different from 101 K/min that we have determined for the 74220,867 orange glass beads. However, the previous calorimetric data, which has a very poor temperature resolution compared to what modern calorimeters are capable of (Uhlmann et al., 1974), suggest an impossible scenario, i.e., a faster cooling rate corresponding to a lower fictive temperature (T_f'). Very little information about the sample characterization and experimental setup has been provided (Uhlmann et al., 1974) and thus it is unclear what may have caused this contradiction.

An alternative way to estimate cooling rates is to numerically model volatile diffusion profiles. The diffusion profiles from the cores to rims detected in individual glass beads are best interpreted as the diffusion having occurred during degassing of the glass beads as they cooled on the Moon's surface (Saal et al., 2008). Cooling rates are included in numerical models of the diffusion profiles preserved in the lunar glass beads. Note that diffusion of volatiles can also be affected by other parameters, such as time to quench (Saal et al., 2008), and the effects of molecular H_2, molecular H_2O and hydroxyl in total H_2O diffusion (Zhang and Stolper, 1991; Zhang, 2011), which were not accounted for in Saal et al. (2008). Nonetheless, the best fits of the diffusion profiles of four different volatile species (H_2O, Cl, F, and S) in individual glass beads suggest an average cooling rate of 120 to 180 K/min (Saal

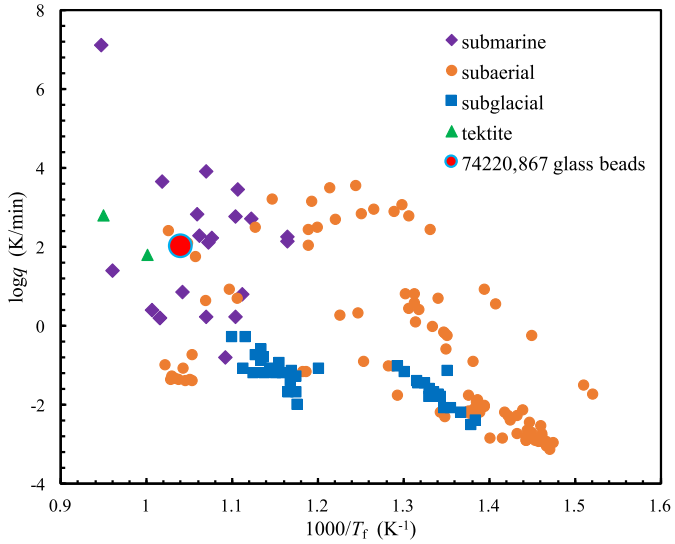

Fig. 5. Comparison of the cooling rates of the 74220,867 lunar orange glass beads with those of terrestrial natural glasses. The data for terrestrial glasses are from: Wilding et al. (2000), Potuzak et al. (2008), and Nichols et al. (2009) for submarine quenched glass; Wilding et al. (1995, 1996a), Gottsmann and Dingwell (2001, 2002), and Xu and Zhang (2002) for subaerial quenched glass; Wilding et al. (2004) for subglacial quenched glass; Wilding et al. (1996b) for tektite.

et al., 2008). The average cooling rate of 101 K/min obtained for 74220,867 volcanic glass beads using calorimeter is close to the lower end of this range. There are two possibilities to account for this small difference. One is that different glass beads may have cooled down at different rates. The second possibility could be that 101 K/min is an average cooling rate of thousands of glass beads at the glass transition. In contrast, the range of cooling rates obtained from volatile diffusion modeling is that above the glass transition (Saal et al., 2008).

5.2. Comparison of cooling rates of natural silicate glasses

Theoretical calculations have shown that cooling media (i.e., environment) and sample size are the most important factors that control the cooling rate of a melt (Birnie and Dyar, 1986). Biot number, a dimensionless quantity, can be used to determine whether the temperatures vary significantly inside the cooling melt. Experiments have demonstrated that for mm-size samples quenched in water, the Biot number of the melt is >1 and the cooling rate is inversely correlated to the distance from the surface within a sample, whereas mm-size and smaller samples quenched in air, the melt Biot number is <0.1 and the cooling rate in each sample is uniform (Xu and Zhang, 2002). Hence, for a small glass bead (typically sub-mm size), the melt cooling rate in each droplet is uniform and controlled by heat transfer in the cooling media instead of heat conduction in the melt. The uniform cooling rate depends on the size of the droplet. In addition, for cooling in a gas medium, the uniform cooling rate also depends on the temperature difference between the droplet and the ambient gas, and the heat transfer coefficient of the gas medium. For cooling in a vacuum, the cooling is by radiation and the rate depends on the emissivity of the droplet.

Laboratory experiments and theoretical calculations have demonstrated that different cooling media result in different glass cooling rates (e.g., Birnie and Dyar, 1986; Xu and Zhang, 2002). Volcanic eruptions on Earth have occurred in different environments. Due to the complexity of natural environments, the terrestrial volcanic glasses have recorded a wide range of cooling rates, over several orders of magnitude (Fig. 5). The cooling rates of glasses recorded for different environments overlap (Fig. 5). Based on the limited data available, cooling rates are highest for submarine volcanic glasses cooled in water, and lower for subaerial and subglacial volcanic glasses. The cooling rate of the 74220,867 volcanic glass beads is close to the upper end of the range of cooling rate of subaerially erupted glasses (0.00072–6.3 K/min of obsidian of Mayor Island, Gottsmann and Dingwell, 2002; 0.0014–4 K/min of volcanic glasses, Wilding et al., 1995; 0.038–0.18 K/min of rhyolite of Lipari, Gottsmann and Dingwell, 2001; 0.0048–600 K/min of Tenerife glasses, Wilding et al., 1996a; 0.24–3300 K/min of pyroclasts of Mono Craters, Xu and Zhang, 2002), as are the cooling rates of tektites (60–600 K/min of tektites, Wilding et al., 1996b) (Fig. 5).

5.3. Estimation of atmospheric conditions on the early Moon

The cooling rate of 101 K/min of the 74220,867 orange volcanic glass beads inferred from their heating C_p curves clearly shows that these glass beads were not cooled in the vacuum that now surrounds the Moon. Cooling rates during "free-flight" in vacuum can be as high as $8 \cdot 10^4$ K/min for melt droplets 160 μm in diameter based on theoretical calculations (Arndt and von Engelhardt, 1987). The physical properties of the cooling media as well as those of the melt will affect the cooling rate (Xu and Zhang, 2002). These properties include thermal conductivity, viscosity and density of the cooling media that are temperature dependent and could have opposite effects on glass cooling rate (e.g., Xu and Zhang, 2002). Therefore, it is difficult to discern the effect of each individual property on glass cooling rate without knowledge of how they are correlated. Nonetheless, based on the comparison between the cooling rates of the 74220,867 glass beads and the terrestrial volcanic glasses, the lunar glass beads were likely quenched in a hot gaseous media (Fig. 5). Geochemical evidence also demonstrates that these lunar volcanic glass beads originated from fire fountain eruptions on the Moon's surface (e.g., Heiken et al., 1974; Meyer et al., 1975; Heiken and McKay, 1977; Reed et al., 1977; Clanton et al., 1978), which is consistent with our inference from the cooling rates of the orange glass beads.

The present lunar atmosphere has a low density and is actually defined as an exosphere (Stern, 1999; Needham and Kring, 2017). However, the results from the heat capacity measurements of 74220,867 glass beads indicate there was at least a short-lived thicker lunar "atmosphere" in the vicinity of the Apollo 17 orange glass eruption. During the early stages of the Moon formation, an early atmosphere may have mainly consisted of volatiles degassed from the crystallizing magma ocean (Saxena et al., 2017). It has also been proposed that degassing from the peak of mare volcanism could have also established a temporary thicker atmosphere (Needham and Kring, 2017) and the peak of such volcanic activity has been estimated to be around 3.5 Ga (Neal, 2017; Needham and Kring, 2017). The existence of gas inferred from the cooling rate of 74220,867 glass beads, which formed at the peak stage of mare volcanism (Huneke, 1978; Tera and Wasserburg, 1976; Neal, 2017), is consistent with (though does not require) such a thicker atmosphere. Therefore, both the lunar magma ocean and mare volcanism may have played important roles in establishing a collisionally thick atmosphere around the Moon at various stages during the early history of the Moon (e.g., Needham and Kring, 2017; Saxena et al., 2017). It is unclear which volatiles were major constituents of the early atmosphere. Volatile metals (Saxena et al., 2017) and CO–S–H_2O (Needham and Kring, 2017) have been proposed and it is possible that the composition of early lunar atmosphere changed both temporally and spatially. However, water has been detected in lunar rocks of different ages, from old ferroan anorthosite to young mare volcanic glass beads, although significant amounts of water were lost due to the degassing of their parental magmas (e.g., Saal et al., 2008; Hui et al., 2013, 2017).

Therefore, water vapor may have been an important component of the early lunar atmosphere.

6. Concluding remarks

The heat capacities of lunar volcanic glass beads collected during the Apollo 17 mission were measured using a differential scanning calorimeter during heating. A cooling rate of 101 K/min was obtained for the 74220,867 orange glass beads. This cooling rate is close to the upper end of the range of cooling rates recorded in volcanic glasses quenched subaerially on Earth's surface (Wilding et al., 1996a; Xu and Zhang, 2002). This suggests that the lunar glass beads were likely cooled in a gas medium released during lunar volcanic events, which indicates that there may have been at least a short-lived thick atmosphere on the early Moon during the peak of volcanic activity around 3.5 Ga.

Acknowledgements

We thank NASA CAPTEM for providing the lunar samples. This research is supported by NSFC grants (41573055 and 41590623) to HH, NASA grants NNX11AH48G to HH, AHP, and YZ, and NNX15AH37G to YZ. We thank the editor William McKinnon, reviewer Helge Gonnermann and an anonymous reviewer for their constructive and detailed comments.

References

Archer, D.G., 1993. Thermodynamic properties of synthetic sapphire (α-Al_2O_3), standard reference material 720 and the effect of temperature-scale differences on thermodynamic properties. J. Phys. Chem. Ref. Data 22, 1441–1453.
Arndt, J., Flad, K., Feth, M., 1979. Radiative cooling experiments on lunar glass analogues. Proc. Lunar Planet. Sci. Conf. 10, 355–373.
Arndt, J., von Engelhardt, W., 1987. Formation of Apollo 17 orange and black glass beads. J. Geophys. Res. 92, E372–E376.
Arndt, J., von Engelhardt, W., Gonzalez-Cabeza, I., Meier, B., 1984. Formation of Apollo 15 green glass beads. J. Geophys. Res. 89, C225–C232.
Birnie, D.P., Dyar, M.D., 1986. Cooling rate calculations for silicate glasses. J. Geophys. Res. 91, D509–D513.
Clanton, U.S., McKay, D.S., Waits, G., Fuhrman, R., 1978. Sublimate morphology on 74001 and 74002 orange and black glassy droplet. Proc. Lunar Planet. Sci. Conf. 9, 1945–1957.
Chen, Y., Zhang, Y., Liu, Y., Guan, Y., Eiler, J., Stolper, E.M., 2015. Water, fluorine, and sulfur concentrations in the lunar mantle. Earth Planet. Sci. Lett. 427, 37–46.
Chou, C.-L., Boynton, W.V., Sundberg, L.L., Wasson, J.T., 1975. Volatiles on the surface of Apollo 15 green glass and trace element distributions among Apollo 15 soils. Proc. Lunar Planet. Sci. Conf. 6, 1701–1727.
DeBolt, M.A., Easteal, A.J., Macedo, P.B., Moynihan, C.T., 1976. Analysis of structural relaxation in glass using rate heating data. J. Am. Ceram. Soc. 59, 16–21.
Delano, J.W., 1986. Pristine lunar glasses: criteria, data, and implications. J. Geophys. Res. 91, D201–D213.
Dingwell, D.B., Webb, S.L., 1990. Relaxation in silicate melts. Eur. J. Mineral. 2, 427–449.
Donaldson, C.H., Drever, H.I., Johnson, R., 1977. Supercooling on the lunar surface: a review of analogue information. Philos. Trans. R. Soc. Lond. A 285, 207–217.
Fang, C.Y., Yinnon, H., Uhlmann, D.R., 1983. Cooling rates for glass containing lunar compositions. J. Geophys. Res. 88S, A907–A911.
Füri, E., Deloule, E., Gurenko, A., Marty, B., 2014. New evidence for chondritic lunar water from combined D/H and noble gas analyses of single Apollo 17 volcanic glasses. Icarus 229, 109–120.
Gottsmann, J., Dingwell, D.B., 2001. The cooling of frontal flow ramps: a calorimetric study on the Rocche Rosse rhyolite flow, Lipari, Aeolian Island, Italy. Terra Nova 13, 157–164.
Gottsmann, J., Dingwell, D.B., 2002. The thermal history of a spatter-fed lava flow: the 8-ka pantellerite flow of Mayor Island, New Zealand. Bull. Volcanol. 64, 410–422.
Heiken, G., McKay, D.S., 1977. A model for eruption behavior of a volcanic vent in eastern Mare Serenitatis. Proc. Lunar Planet. Sci. Conf. 8, 3243–3255.
Heiken, G.H., McKay, D.S., Brown, R.W., 1974. Lunar deposits of possible pyroclastic origin. Geochim. Cosmochim. Acta 38, 1703–1718.
Hui, H., Peslier, A.H., Zhang, Y., Neal, C.R., 2013. Water in lunar anorthosites and evidence for a wet early Moon. Nat. Geosci. 6, 177–180.
Hui, H., Guan, Y., Chen, Y., Peslier, A.H., Zhang, Y., Liu, Y., Flemming, R.L., Rossman, G.R., Eiler, J.M., Neal, C.R., Osinski, G.R., 2017. A heterogeneous lunar interior for hydrogen isotopes as revealed by the lunar highlands samples. Earth Planet. Sci. Lett. 473, 14–23.
Huneke, J.C., 1978. ^{40}Ar–^{39}Ar microanalysis of single 74220 glass balls and 72435 breccia clasts. Proc. Lunar Planet. Sci. Conf. 9, 2345–2362.
Meyer Jr., C., McKay, D.S., Anderson, D.H., Butler Jr., P., 1975. The source of sublimates on the Apollo 15 green and Apollo 17 orange glass samples. Proc. Lunar Planet. Sci. Conf. 6, 1673–1699.
Moynihan, C.T., Easteal, A.J., DeBolt, M.A., 1976. Dependence of the fictive temperature of glass on cooling rate. J. Am. Ceram. Soc. 59, 12–16.
Narayanaswamy, O.S., 1971. A model of structural relaxation in glass. J. Am. Ceram. Soc. 54, 491–498.
Narayanaswamy, O.S., 1988. Thermorheological simplicity in the glass transition. J. Am. Ceram. Soc. 71, 900–904.
Neal, C.R., 2017. Lunar LIPs: What story are they telling us? Lunar Planet. Sci. Conf. Abstr. 48, #1912.
Needham, D.H., Kring, D.A., 2017. Lunar volcanism produced a transient atmosphere around the ancient Moon. Earth Planet. Sci. Lett. 478, 175–178.
Ni, P., Zhang, Y., Guan, Y., 2017. Volatile loss during homogenization of lunar melt inclusions. Earth Planet. Sci. Lett. 478, 214–224.
Nichols, A.R.L., Potuzak, M., Dingwell, D.B., 2009. Cooling rates of basaltic hyaloclastites and pillow lava glasses from the HSDP2 drill core. Geochim. Cosmochim. Acta 73, 1052–1066.
Nyquist, L.E., 1977. Lunar Rb–Sr chronology. Phys. Chem. Earth 10, 103–142.
Ochs, F.A., Lange, R.A., 1997. The partial molar volume, thermal expansivity, and compressibility of H_2O in silicate melts: new measurements and an internally consistent model. Contrib. Mineral. Petrol. 129, 155–165.
Potuzak, M., Nichols, A.R.L., Dingwell, D.B., Clague, D.A., 2008. Hyperquenched volcanic glass from Loihi Seamount, Hawaii. Earth Planet. Sci. Lett. 270, 54–62.
Reed Jr., G.W., Allen, R.O., Jovanovic, S., 1977. Volatile metal deposits on lunar soils – relation to volcanism. Proc. Lunar Planet. Sci. Conf. 8, 3917–3930.
Roedder, E., Weiblen, P.W., 1973. Apollo 17 "orange soil" and meteorite impact on liquid lava. Nature 244, 210–212.
Rutherford, M.J., Papale, P., 2009. Origin of basalt fire-fountain eruptions on Earth versus the Moon. Geology 37, 219–222.
Saal, A.E., Hauri, E.H., Lo Cascio, M., Van Orman, J.A., Rutherford, M.C., Cooper, R.F., 2008. Volatile content of lunar volcanic glasses and the presence of water in the Moon's interior. Nature 454, 192–195.
Saxena, P., Elkins-Tanton, L., Petro, N., Mandell, A., 2017. A model of the primordial lunar atmosphere. Earth Planet. Sci. Lett. 474, 198–205.
Shearer, C.K., Hess, P.C., Wieczorek, M.A., Pritchard, M.E., Parmentier, E.M., Borg, L.E., Longhi, J., Elkins-Tanton, L.T., Neal, C.R., Antonenko, I., Canup, R.M., Halliday, A.N., Grove, T.L., Hager, B.H., Lee, D.-C., Wiechert, U., 2006. Thermal and magmatic evolution of the Moon. Rev. Mineral. Geochem. 60, 365–518.
Spangler, R.R., Warasila, R., Delano, J.W., 1984. ^{39}Ar–^{40}Ar ages for the Apollo 15 green and yellow volcanic glasses. J. Geophys. Res. 89, B487–B497.
Stern, A.A., 1999. The lunar atmosphere: history, status, current problems, and context. Rev. Geophys. 37, 453–491.
Tatsumoto, M., Premo, W.R., Unruh, D.M., 1987. Origin of lead from green glass of Apollo 15426: a search for primitive lunar lead. J. Geophys. Res. 92, E361–E371.
Tera, F., Wasserburg, G.J., 1976. Lunar ball games and other sports. Lunar Planet. Sci. Conf. Abstr. 7, 858–860.
Tool, A.Q., 1946. Relation between inelastic deformability and thermal expansion of glass in its annealing range. J. Am. Ceram. Soc. 29, 240–253.
Uhlmann, D.R., Klein, L., Kritchevsky, G., Hopper, R.W., 1974. The formation of lunar glasses. Geochim. Cosmochim. Acta, Suppl. 5, 2317–2331.
Uhlmann, D.R., Yinnon, H., Fang, C.-Y., 1981. Simplified model evaluation of cooling rates for glass-containing lunar compositions. Proc. Lunar Planet. Sci. Conf. 12B, 281–288.
Wilding, M.C., Webb, S.L., Dingwell, D.B., 1995. Evaluation of a relaxation geospeedometer for volcanic glasses. Chem. Geol. 125, 137–148.
Wilding, M., Webb, S., Dingwell, D., Ablay, G., Marti, J., 1996a. Cooling rate variation in natural volcanic glasses from Tenerife, Canary Islands. Contrib. Mineral. Petrol. 125, 151–160.
Wilding, M., Webb, S., Dingwell, D.B., 1996b. Tektite cooling rates: calorimetric relaxation geospeedometry applied to a natural glass. Geochim. Cosmochim. Acta 60, 1099–1103.
Wilding, M., Dingwell, D., Batiza, R., Wilson, L., 2000. Cooling rates of hyaloclastites: applications of relaxation geospeedometry to undersea volcanic deposits. Bull. Volcanol. 61, 527–536.
Wilding, M.C., Smellie, J.L., Morgan, S., Lesher, C.E., Wilson, L., 2004. Cooling process recorded in subglacially erupted rhyolite glasses: rapid quenching, thermal buffering, and the formation of meltwater. J. Geophys. Res. 109, B08201. https://doi.org/10.1029/2003JB002721.
Xu, Z., Zhang, Y., 2002. Quench rates in air, water, and liquid nitrogen, and inference of temperature in volcanic eruption columns. Earth Planet. Sci. Lett. 200, 315–330.
Yue, Y., Christiansen, J.d.C., Jensen, S.L., 2002. Determination of the fictive temperature for a hyperquenched glass. Chem. Phys. Lett. 357, 20–24.
Zhang, Y., 2011. "Water" in lunar basalts: the role of molecular hydrogen (H_2), especially in the diffusion of the H component. Lunar Planet. Sci. Conf. Abstr. 42, #1957.
Zhang, Y., Stolper, E.M., 1991. Water diffusion in basaltic melts. Nature 351, 306–309.